Eur. Phys. J. D **9**, 565–570 (1999)

THE EUROPEAN PHYSICAL JOURNAL D

EDP Sciences

Structural transformations in II-VI semiconductor nanocrystals

C. Ricolleau[1], L. Audinet[1], M. Gandais[1], and T. Gacoin[2]

[1] Laboratoire de Minéralogie-Cristallographie de Paris, Universités Paris 6 et Paris 7, CNRS UMR 7590, Case 115, 4 Place Jussieu, F-75252 Paris Cédex 05, France
[2] Laboratoire de Physique de la Matière Condensée, Ecole Polytechnique, F-91128 Palaiseau Cédex, France

Received: 1 September 1998 / Received in final form: 4 October 1998

Abstract. Colloidal CdS and CdS/ZnS nanostructures were obtained by nucleation and growth in colloidal solution. Their mean sizes range between 3 and 10 nm. The structural properties were studied by the use of high-resolution transmission electron microscopy (HRTEM). Phase transition between the metastable cubic blende-type structure and the stable hexagonal wurtzite-type structure was evidenced to be a function of the size of the CdS clusters. The mechanism of the transition involving stacking faults was determined by the heating of CdS clusters at 200 °C for 30 h. Results concerning structural relations between CdS and ZnS that occur during the epitaxial growth of ZnS on the CdS nanocrystals showed the existence of the hexagonal structure of ZnS, which is the high-temperature phase of ZnS.

PACS. 61.46.+w Clusters, nanoparticles, and nanocrystalline materials – 68.35.Rh Phase transitions and critical phenomena – 61.16.Bg Transmission, reflection and scanning electron microscopy (including EBIC)

1 Introduction

There has been a great interest in II-VI semiconductor nanocrystals since the pioneering work of Jain and Linde [1], who reported a high value of the third-order susceptibility $\chi^{(3)}$, which controls the nonlinear optical properties of these materials. This interest has been justified by the discovery that there are original optical properties related to the confinement of charge carriers when the particle size is of the order of magnitude of the Bohr radius of the exciton. A number of works have been devoted to fundamental as well as technological aspects of such materials. For both points of view, it is necessary to be able to control the synthesis of materials with well-defined structural properties, e.g., crystal structure, particle mean size, size distribution. It is also important to get detailed information about features that play a role in the physical properties of the clusters, such as defects, morphology, and surface of the nanocrystal. The last point is of particular interest, since the surfaces of small particles include a large ratio of atoms in comparison with the volume: around 25% for a cube of 2 nm. For this reason, surfaces play a role, not only in nucleation and growth processes, but also in physical and chemical properties. The present paper deals with CdS and CdS/ZnS colloidal nanostructures produced by the use of the technique of inverted micelles [2]. They have been studied by high-resolution transmission electron microscopy (HRTEM). Their structures have been followed as a function of their size and the temperature. After a brief description of the production process, results concerning the structural properties and the mechanism of phase transformation occurring in the CdS clusters will be presented. The last part of the paper is devoted to the structural relations between CdS and ZnS involved in the epitaxial growth of ZnS on CdS.

2 Experimental details

2.1 Preparation of the nanocrystals

Inverted micelles are nanodrops of water dispersed in heptane and stabilized in this liquid by a cap of surfactant molecules. Their mean size depends on the ratio of [water]/[surfactant]. A solution of inverted micelles containing cadmium nitrate is prepared, and hydrogen sulphide is injected. A very fast reaction between Cd^{2+} and S^{2-} ions occurs in the micelles, giving rise to the formation of CdS nanocrystals with mean size controlled by both the micelles' mean size and the amount of Cd^{2+} ions [3]. Next, for the preparation of the CdS/ZnS nanostructures, the coating of ZnS was obtained by introducing Zn^{2+} and S^{2-} ions in the solution [4]. Nanocrystals were separated from the micelles by the addition of organic molecules, such as pyridine, that graft at the surface of the nanocrystals and induce their precipitation. All these reactions take place at room temperature. Nanocrystals were extracted from the solution in two steps of the synthesis, before and after the introduction of Zn^{2+} ions, so that the CdS clusters and the CdS/ZnS nanostructures could be studied.

2.2 Structural analysis

For electron microscopy studies, the powder of nanocrystals was dissolved in aceton, and a drop of the solution was deposited on a carbon thin film. HRTEM was performed with a Philipps EM430 ST electron microscope operating at 300 kV with point-to-point resolution of 0.20 nm. HRTEM micrographs were magnified and digitized with 512×512 pixels and 1024 grey levels by an air-cooled CCD camera. The magnification used for the digitization was chosen so that one pixel would correspond to a dimension smaller than the spatial resolution of the microscope. The structural analysis of the clusters was achieved by examination of the power spectrum (i.e., $|\text{Fourier transform}|^2$) of the HRTEM images of nanocrystals seen along the zone axis. The spectrum exhibits characteristic features which allow an unambiguous identification of the crystallographic structure.

3 Results

3.1 CdS nanocrystal structures

Depending on the size of the CdS clusters, different structures have been identified: (i) In the first stage of the growth (i.e., when the size is smaller than 3–4 nm), CdS are mainly crystallized in the metastable cubic structure of blende type (the B structure). This phase, which occurs in the early stage of the growth, is favoured by the nucleation kinetics [5, 6]. (ii) In later stages (i.e., when the size is larger than about 7–8 nm), they are in the stable hexagonal structure of wurtzite type (the W structure). (iii) In between, they are in intermediate phases consisting of either the B structure with stacking faults and twins (Fig. 1a) or in associations of B and W domains sharing a close-packed atomic layer (Fig. 1b). These results corroborate the structural analysis of colloidal CdSe nanocrystals deduced from X-ray diffraction by Bawendi *et al.* [7]. These experiments clearly show that the phase transition between cubic and hexagonal modifications of CdS clusters is induced by a size effect. The larger the crystal, the lower is its surface energy contribution to the total free energy of the cluster; the stable hexagonal structure of CdS is thus favoured.

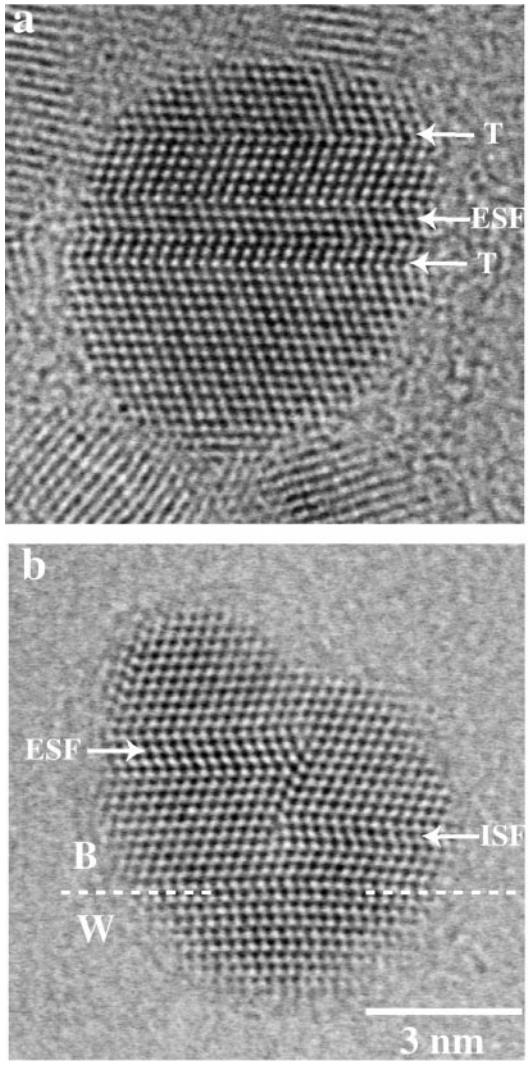

Fig. 1. HRTEM images of CdS clusters in the B-type structure seen along the [110] zone axis: (a) faulted B-type cluster; (b) two-phase cluster showing the coexistence of B- and W-type structures. ISF: Intrinsic stacking fault. ESF: Extrinsic stacking fault. T: Twin boundary.

3.2 Structural defects and two-phase nanostructures

The blende and wurtzite structures are the two types of atomic arrangements adopted by tetrahedral coordinated semiconductors of the III-V and II-VI groups. The lattice is FCC in the B structure and CPH in the W structure. According to the usual description, each structure is composed of two sublattices displaced from each other by $\frac{1}{4}\langle 111\rangle$ and $\frac{1}{8}[0001]$ in B and W structures, respectively, Cd atoms being at the nodes of one lattice and S atoms at the nodes of the other lattice. Each atom of one species is bonded to four atoms of the other species. As is well known, B and W structures have double layers of close-packed atomic planes (each layer being composed of one Cd plane and one S plane). They differ by the stacking sequence of these layers: A-aB-bC-cA-aB-bC-c... for the B structure and A-aB-bA-aB-b... for the W structure, where capital letters denote pure Cd planes and small letters pure S planes or the opposite. Atoms of different species are triply bonded within double layers, such as a-B, b-C, and c-A, and they are singly bonded between double layers such as A-a, B-b, and C-c. We may notice that such structures are polar in the directions normal to close-packed planes, namely any of the four $\langle 111\rangle$ directions in the B structure and the [0001] direction in the W structure.

In the case of these structures, two-phase nanostructures could be formed by the stacking of one, two, or more stacking faults and/or twin boundaries, because these de-

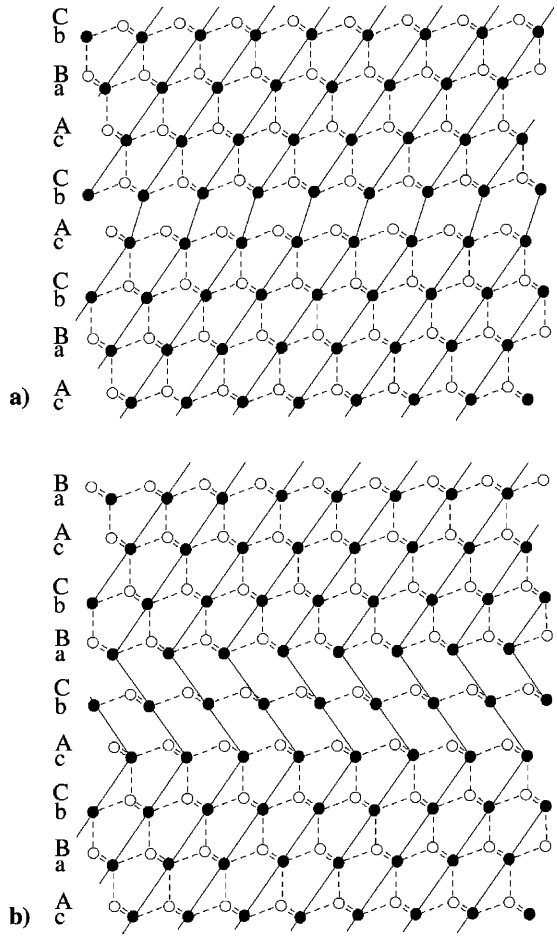

Fig. 2. Schematization of the stacking sequence in the blende structure in the case of: (a) intrinsic stacking fault; (b) extrinsic stacking fault (White circle: S atoms; black circle: Cd atoms or the reverse).

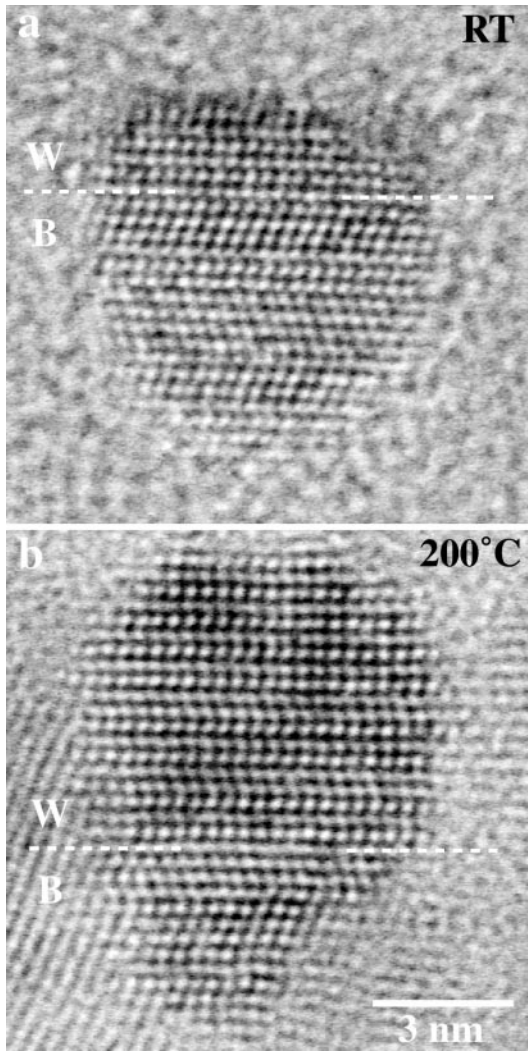

Fig. 3. Evolution of the two-phase nanostructure as a function of temperature: (a) room temperature; (b) $T = 200\,^{\circ}\mathrm{C}$. The respective part of the clusters in B- and W-type phases are separated by the dashed line.

fect families can be also described as thin layers of wurtzite introduced in the B structure. In the B structure, stacking faults and twins occur on {111} planes. They involve bond modifications only on the neighbours that are fourth nearest. Stacking faults are obtained by a $\frac{1}{6}\langle 112\rangle$ glide of close-packed planes. Two kinds of stacking faults may be distinguished. The first one gives rise to the sequence ...-cA-aB-bC-cA-bC-cA-aB-bC-... It is the so-called intrinsic stacking fault (ISF): it can be described by the absence of a double layer. The ISF is schematized in Fig. 2a, and the corresponding experimental case is shown in Fig. 1b (the fault is indicated by the arrow labelled ISF). The other kind of stacking fault gives the sequence ...-cA-aB-bC-cA-bC-aB-bC-cA-aB-..., corresponding to an extrinsic stacking fault (ESF), which can be described by the introduction of a layer. This fault can be also described as two twin planes separated by two atomic layers, as can be clearly observed in Figs. 1a and 1b, where the fault is underlined by the arrow labelled ESF. An ideal scheme of ESF is drawn on Fig. 2b. Twins of low energy on {111} planes may occur by rotation of 180° around the ⟨111⟩ axis and induce the sequence ...cA-aB-bC-cB-bA-aC-... (Fig. 1a: the twin boundary is indicated by the arrow labelled T). Rotation twin keeps the stacking of close-packed planes of atoms of different species across the twin boundary and does not modify the polarity of the structure.

3.3 Blende → wurtzite phase transformation

To identify the mechanism of phase transformation between the two phases of CdS (Sect. 3.1), we annealed for 30 h at 200 °C a sample containing CdS clusters. The mean size of the clusters was around 5 nm. The following results are summarized in Table 1. At room temperature, the clusters with B structure were predominant (57%) in comparison with those with a W structure (39%). After the annealing, this tendency reversed completely: The clusters now had mainly a W structure (60%), and the number of

Table 1. Evolution of the crystalline state (in % of the different phases) before and after the thermal annealing of CdS clusters during 30 h at 200 °C.

Structure	Before annealing	After annealing
Blende	41	12
Faulted blende	16	16
Two-phase nanostructure	4	12
Wurtzite	39	60

crystals with B structure was largely reduced (28%). It is notable that there was an increase by a factor of 3 in the number of the crystals in the two-phase state, parallel to this evolution.

Furthermore, the volume fraction of the W phase significantly increased after the annealing: before annealing, the W phase occupied $\frac{1}{4}$ of the whole crystal (Fig. 3a), whereas at $T = 200\,^{\circ}\mathrm{C}$, this fraction becomes $\frac{2}{3}$ of the crystal (Fig. 3b). In the two-phase nanostructure, the wurtzite structure appears in projection along the **a** axis (Figs. 3a and 3b). This projection displays effects of the 6_3 symmetry axis in dynamical conditions of diffraction. The odd reflections (i.e., 0001) along the $\mathbf{c}^*$ axis, forbidden by 6_3 symmetry, are effectively extinct when the **a** axis is strictly parallel to the electron beam: The lattice pattern then displays the $\frac{c}{2}$ periodicity (Fig. 3a and middle of the crystal in Fig. 3b). The extinction laws can be transgressed by the double diffraction effect when the zone axis is misaligned: The periodicity is then c (top of the crystal in Fig. 3b).

As we have seen in Sect. 3.2, stacking faults may also be considered as thin layers of wurtzite structure introduced in the blende structure. In such a way, the development of wurtzite layers within the blende structure can proceed by the creation and glide of partial dislocations in order to create stacking faults: Two or more stacking faults then form nanodomains of W structure. This mechanism involving only glide motions of atoms is at the origin of the B $\rightarrow$ W phase transition during the growth.

3.4 Core/shell CdS/ZnS nanostructures

Evidence of core/shell nanostructure was obtained by a through-focus series of images of a crystal. Images of W- and B-type crystals were clear and gave precise information on the growth of ZnS on CdS. When the two materials were juxtaposed, as was the case in the two examples presented in Fig. 4, different contrasts could be seen between the inner and the outer parts of the nanostructures. These contrasts were obtained by the variation of the defocus of the objective lens, which modifies the interference conditions between the transmitted and the diffracted beams. For example, for the crystals in Fig. 4, the ZnS coating layer could be imaged or not, depending on the value of the focus and the thickness of the layer.

In the wurtzite case (Figs. 4a and 4b), direct evidence of the growth of ZnS on the $\{11\bar{2}0\}$ prismatic faces was obtained by way of a Fourier transform (FT) of experimental images of the core/shell nanostructure when the whole crystal is imaged. The FT of the crystal presented in Fig. 4a is shown in Fig. 4c. It has two main features. The first one is the epitaxial relationship between the CdS core and the ZnS layer:

$$\{11\bar{2}0\}_{\mathrm{CdS}}//\{11\bar{2}0\}_{\mathrm{ZnS}} \quad \text{and} \quad [10\bar{1}0]_{\mathrm{CdS}}//[10\bar{1}0]_{\mathrm{ZnS}}$$

The second notable feature of FT is that it allows us to determine the structure of the ZnS layer, which is a hexagonal one of the W type. Finally, the mismatch between two equivalent reflections gives a value of 7%.

In the blende case (Figs. 4d and 4e), the core crystal was completely coated by a shell layer, which has the same B-type structure as the core but has a lattice spacing that is 7.1% smaller (Fig. 4f). This is true for both families of {111} planes, which are parallel to the CdS/ZnS boundary and inclined at the angle of 70°. The difference of 7% between core and shell lattice parameters measured in both cases (W and B structures) corresponds to the difference of the lattice parameters between bulk CdS and ZnS materials.

These results show that the structure of the ZnS epitaxial layer is imposed by the CdS core, giving rise to the formation of ZnS in the hexagonal W-type structure, which is stable, in the case of the bulk material, only at high temperature. Secondly, the thickness of the ZnS epitaxial layer overcomes the limit value, allowing the accommodation of core/shell lattice misfit by elastic strain. The elastic strain was relaxed by the formation of dislocations in the CdS/ZnS boundary plane (indicated by the arrows labelled D in Figs. 4a and 4d).

4 Conclusion

The determination of the crystal structure of CdS clusters was performed by the use of high-resolution electron microscopy. In early stages of the nucleation and growth process (at sizes smaller than 3–4 nm), the crystals had mainly a metastable cubic structure, of the B type, because of a competition between surface and volume energies. Two-phase nanostructures have been evidenced, and the role of structural defects in the metastable cubic phase of the B type involved in the blende $\rightarrow$ wurtzite phase transformation has been clearly demonstrated. These results have allowed us to show that the metastable cubic phase progressively transforms into the W-type stable structure of during the growth. Finally, the inverted micelle technique appears to be very promising for the synthesis of CdS/ZnS nanostructures. The conditions used in the present work (i.e., room temperature and the micelle size of around 5 nm) have favoured the epitaxial growth of ZnS on CdS nanocrystals, with an abrupt boundary. The thickness of the epitaxial layer is

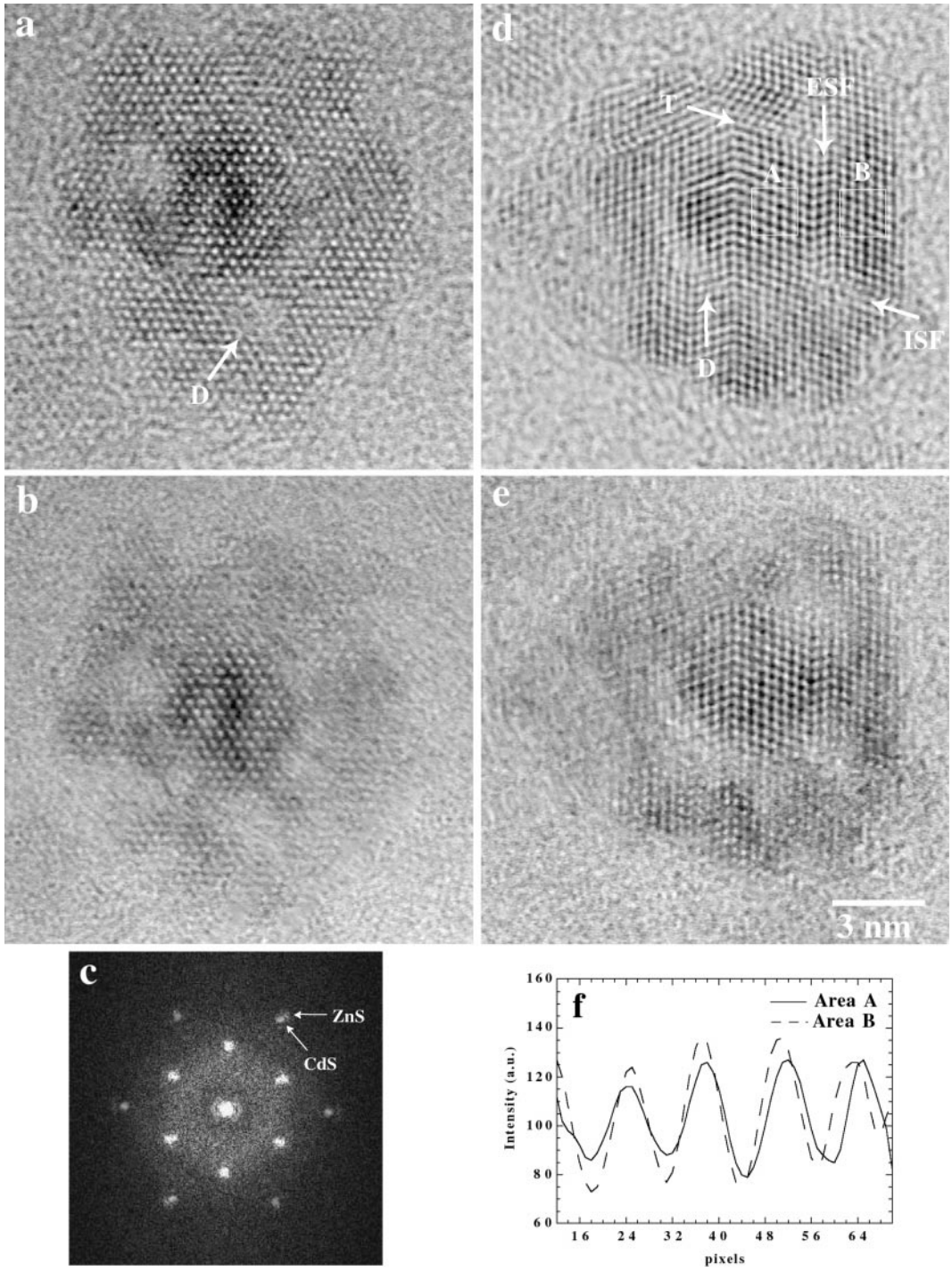

Fig. 4. HRTEM images of CdS/ZnS core/shell nanostructures in: ● Wurtzite structure: (a) whole crystal seen along the [0001] zone axis; (b) core crystal seen along the same axis; (c) Fourier transform of the image (a), exhibiting the epitaxial relationship between ZnS and CdS. ● Blende structure: (d) whole crystal seen along the [110] zone axis; (e) core crystal seen along the same axis; (f) intensity profiles of the fringes corresponding to the {111} planes (plain line: CdS core crystal, area A; dashed line: ZnS shell layer, area B). The arrows labelled D indicate dislocations.

in the 1.3–2 nm range, and the structure of the ZnS layer is imposed by the one of the CdS core; this gives rise to the formation of a ZnS layer in the hexagonal structure, which is the high-temperature stable phase of the bulk material.

References

1. R.K. Jain, R.C. Lind: J. Opt. Soc. Am. **73**(5), 647 (1983)
2. P. Lianos, J.K. Thomas: Chem. Phys. Lett. **125**, 299 (1986)

3. T. Gacoin, C. Train, F. Chaput, J.P. Boilot, P. Aubert, M. Gandais, Y. Wang, A. Lecomte: SPIE Sol-Gel Opt. **1758**, 565 (1992)
4. T. Gacoin, L. Malier, G. Counio, S. Esnouf, J.P. Boilot, L. Audinet, C. Ricolleau, M. Gandais: Mater. Res. Soc. Symp. Proc. **435**, 643 (1996)
5. C. Ricolleau, L. Audinet, M. Gandais, T. Gacoin, J.P. Boilot, M. Chamarro: J. Cryst. Growth **159**, 861 (1996)
6. B. Mutaftschiev: in *Handbook of Crystal Growth*, ed. by D.T.J. Hurle (North-Holland, Amsterdam 1993)
7. M.G. Bawendi, A.R. Kortan, M.L. Steigerwald, L.E. Brus: J. Chem. Phys. **91**(11), 7282 (1989)